AIP | Applied Physics Letters

Improvement of redox reactions by miniaturizing nanoparticles of zinc Prussian blue analog

Kyoung Moo Lee, Hisashi Tanaka, Kyung Ho Kim, Midori Kawamura, Yoshio Abe et al.

Citation: Appl. Phys. Lett. **102**, 141901 (2013); doi: 10.1063/1.4800443
View online: http://dx.doi.org/10.1063/1.4800443
View Table of Contents: http://apl.aip.org/resource/1/APPLAB/v102/i14
Published by the American Institute of Physics.

Improvement of redox reactions by miniaturizing nanoparticles of zinc Prussian blue analog

Kyoung Moo Lee,[1,2] Hisashi Tanaka,[1] Kyung Ho Kim,[2] Midori Kawamura,[2] Yoshio Abe,[2] and Tohru Kawamoto[1,a)]

[1]*Nanosystem Research Institute, National Institute of Advanced Industrial Science and Technology (AIST), 1-1-1 Higashi, Tsukuba, Ibaraki 305-8565, Japan*

[2]*Department of Materials Science and Engineering, Kitami Institute of Technology, Kitami, Hokkaido 090-8507, Japan*

(Received 1 March 2013; accepted 24 March 2013; published online 8 April 2013)

We demonstrated the redox reaction improvement of zinc-Prussian blue analogues (ZnPBA: zinc hexacyanoferrate) by size-controlled nanoparticles after centrifuge classification. The average size in the smallest class was 58.8 nm. With size-controlled ZnPBA nanoparticles, dense thin films can be fabricated with no binding material. These films show stable redox cycling even after 10 000 cycles. Results show that size-controlled ZnPBA nanoparticle films are promising candidates for use as counter-electrode materials for nonvolatile electrochromic devices. © *2013 American Institute of Physics*. [http://dx.doi.org/10.1063/1.4800443]

Electrochromism, reversible color changes of electroactive materials on redox reactions, has attracted keen interest because of their potential application to various devices. For example, electrical color-switchable glasses to control light transmission have been commercialized for use in aircraft windows.[1] Energy-saving in buildings and automobiles is also fascinating applications of electrochromic devices (ECDs). ECDs have also been investigated for application to information display devices such as electronic paper, with extremely low energy consumption.[2,3]

Some ECDs have a nonvolatile effect, i.e., maintaining color without electricity, which is an important property for energy-saving applications.[4] Usually, nonvolatile ECDs have layered structures with anodic and cathodic electroactive layers resembling those of a Li-ion battery. With the layered structure, the redox state is maintained under the open circuit situation. When we hope to use ECDs for windows, a colorless counter-layered electrode with no color in both oxidized and reduced states is necessary, because an ECD with such a counter-electrode shows the same color change as the EC layer.

As materials for the nonvolatile ECD, Prussian blue ($A_yFe[Fe(CN)_6]_x$, PB) and its analogues have been fascinating because of their excellent properties of cycling stability, fast response, and low cost.[5–11] PB changes its color to dark blue by oxidation and becomes transparent by reduction. Furthermore, when using dispersible Prussian blue nanoparticles, an electrochromic layer can be fabricated easily using coating/printing techniques.[12]

$A_yZn[Fe(CN)_6]_x$ (ZnPBA), a Prussian blue analogue, is a candidate for use as a colorless counter-electrode. It is nearly colorless in both oxidized and reduced states, and is more cost-effective than other PB analogues.[13] With the combination of PB and ZnPBA, the ECD exhibits a color change resembling that of PB's electrochromism. However, ZnPBA presents difficulties because of its lower cycling stability.[13,14] The addition of conducting polymers with ZnPBA in the thin film fabrication reportedly improves the cycling stability.[13,14] However, some problems persist, which require lowering of the transmittance and the cost. This study was conducted to clarify the conditions for fabrication of ZnPBA thin film exhibiting stable redox reaction with no binding materials.

The large particle size of the ZnPBA nanoparticle (ZnPBA-NP) might explain its low cycling stability. The typical particle size of the ZnPBA-NP is 200–500 nm.[13] In contrast, the size of the PB nanoparticle used was less than 100 nm.[2,10,12,15–17] Especially, Kurihara *et al.*[12] reported nanoparticle synthesis methods that are environmentally friendly, inexpensive, and compatible with various PB analogues. For example, the particle size of the water-dispersible PB nanoparticle is estimated as 10 nm.[3]

This report explains the preparation of ZnPBA-NP with particles smaller than 100 nm. Additionally, we demonstrate that such a small ZnPBA-NP thin film shows a stable redox reaction compared with thin films produced with larger particles. First, we prepared water-dispersible ZnPBA-NP dispersion liquid using Kurihara's methods.[15] The ZnPBA-NP was classified into some components with different sizes using centrifuge processes. The effects of the particle size on electrochemical stability and transferred charge density of Zn-PBA films were examined to clarify their potential as counter-electrodes of ECDs.

The synthesis methods of water-dispersible ZnPBA-NP resemble those for PB nanoparticles: 300 ml aqueous solution of 21.8 g of $ZnCl_2$, 5 ml of 10 wt. % HCl, and 300 ml aqueous solution of 38.8 g $Na_4[Fe(CN)_6]\cdot 10H_2O$ were vigorously stirring for 5 min using a homogenizer. The resulting white precipitate was washed with deionized (DI) water five times with a centrifuge to yield the insoluble Zn-PBA precursor. Then, 200 ml aqueous solution of 11.62 g $Na_4[Fe(CN)_6]\cdot 10H_2O$ was added to the ZnPBA precursor, stirring at room temperature for 1 day. After drying, the as-synthesized ZnPBA-NPs were obtained. The three kinds of size-controlled ZnPBA-NPs were obtained as precipitates by centrifuge of the dispersion liquid of the as-synthesized

a)Electronic mail: tohru.kawamoto@aist.go.jp

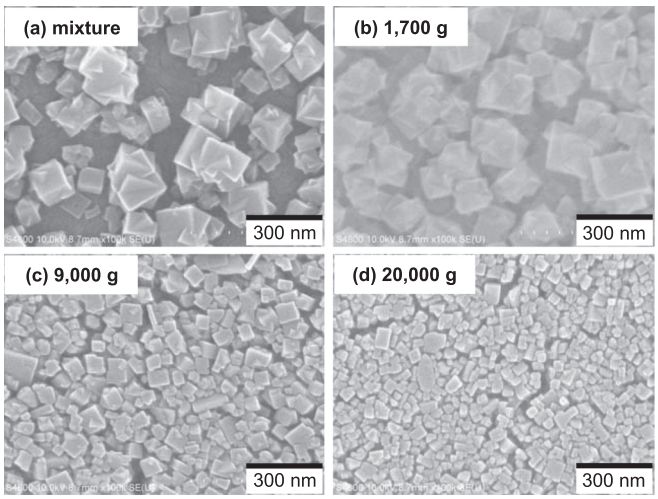

FIG. 1. Top-view FE-SEM images of the size-controlled ZnPBA-NP films on ITO substrates. (a) mixture, (b) 1,700 g, (c) 9,000 g, (d) 20,000 g; where g represents the gravitational acceleration unit.

TABLE I. Particle size distribution and average particle size, d_{avg}, of ZnPBA-NP. The distribution was measured from FESEM images. The average particle sizes are obtained from DLS measurement with each 0.1 g/ml dispersion liquid.

Sample	Particle size distribution (nm)	d_{avg} (nm)
Mixture	20–250	182.9
1700 g	100–250	214.0
9000 g	30–80	70.6
20 000 g	20–60	58.8

ZnPBA-NP at 1700 g, 9000 g, and 20 000 g, respectively, where g represents the gravitational acceleration unit.

Thin films of each ZnPBA-NP sample were produced on indium tin oxide (ITO)/glass substrates using spin-coating with the dispersion liquid of each ZnPBA-NP at a concentration of 0.1 g/ml. The film thickness was controlled using the spin-coater rotation rate. The film particle size and morphology were observed using a field emission scanning electron microscope (FESEM, S-4800II; Hitachi Ltd., Japan). The average particle size was also measured using dynamic light-scattering (DLS) measurement (DelsaNano HC Particle Analyzer, Beckman Coulter, Inc., Ireland). The film thicknesses measured from cross-sectional FESEM images were 202–274 nm. Their electrochemical properties were characterized in 0.1M potassium bis (trifluoromethanesulfonyl) imide/propylene carbonate electrolyte. Saturated calomel electrode (SCE), Pt wire, and ZnPBA films were used, respectively, for reference, counter, and working electrodes. The working electrode area was set to 1.0 cm^2.

The size-control of the ZnPBA-NP was conducted using the centrifuge process. The difference of particle sizes is readily apparent in the FESEM images of films presented in Fig. 1. The particle size for the mix ZnPBA-NP from FESEM images is very widely distributed from 20 nm to 250 nm, as shown in the center column in Table I. In contrast, films of ZnPBA-NP prepared using centrifuge separation have a narrow range of size distribution, as presented in Figs. 1(b)–1(d). The acceleration in the centrifuge process is greater, thereby creating smaller particles. Results also show that separated ZnPBA-NP films have a dense structure. A similar tendency is found in the average particle size in the dispersion liquid, as shown in the right column in Table I.

Improved electrochemical properties are found with the thin film of the smaller ZnPBA-NP. A cyclic voltammogram for each ZnPBA-NP films is presented in Fig. 2, where a pair of main peaks is observed because of the redox reaction of the surface confined iron centers ($Fe^{II/III}$).[18] Acceleration of the redox reaction by the use of smaller particles is found in the difference in the redox potential and current density between oxidized/reduced reactions: The smaller particles have correspondingly smaller differences of the redox potentials, with higher current density, which might result from shortening of the ion-diffusion path in the nanoparticles in the small ZnPBA-NPs.

The cycle stability is also better in smaller particles. The transferred charge density during oxidized and reduced reaction in each cycle of the ZnPBA-NP films is depicted in Fig. 3. The transferred charge density is drastically lower during the initial 500 cycles for the film prepared by mixture (as-synthesized ZnPBA-NP). By contrast, the thin films of the small classes of ZnPBA-NP maintain a larger transferred charge density, even up to 2500 cycles.

The cycle stability of the thin film of the smallest class of ZnPBA-NP with $d_{avg} = 58.8$ nm showed superior electrochemical properties. The film was investigated further up to 10 000 cycles, as portrayed in Fig. 4. In this case, 80% of the initial charge capacity was maintained even after 10 000 cycles. Consequently, the downsized ZnPBA-NP films are

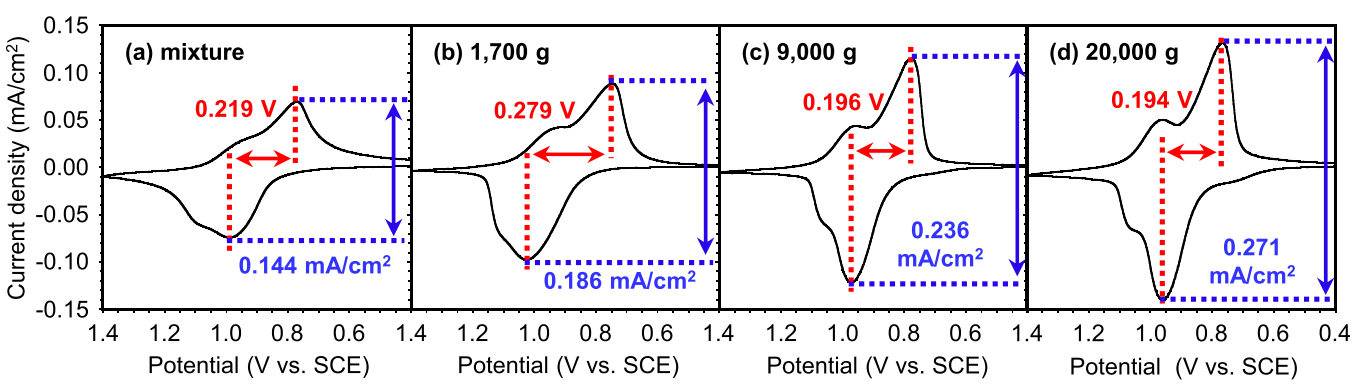

FIG. 2. Initial cyclic voltammograms for the size-controlled ZnPBA-NP films.

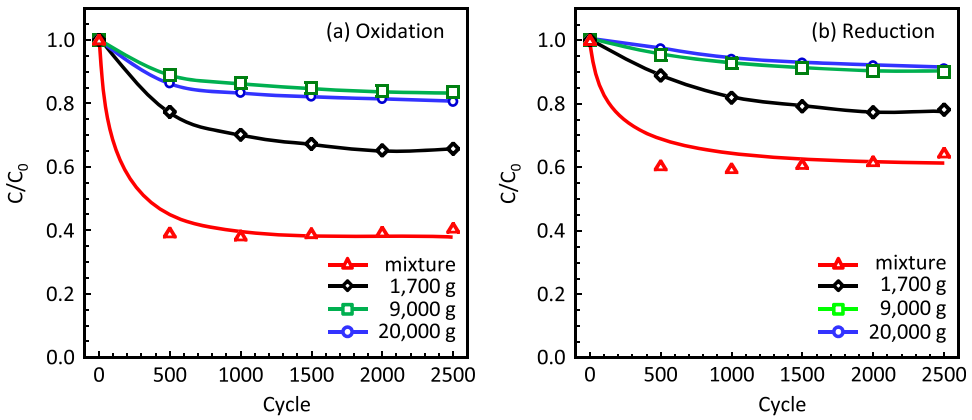

FIG. 3. Cycle stability of transferred charge density for the ZnPBA-NP films after (a) oxidation at 1.4 V and (b) reduction at 0.4 V for 15 s. C_0 and C, respectively, indicate the transferred charge density at the initial cycle and those after cycles.

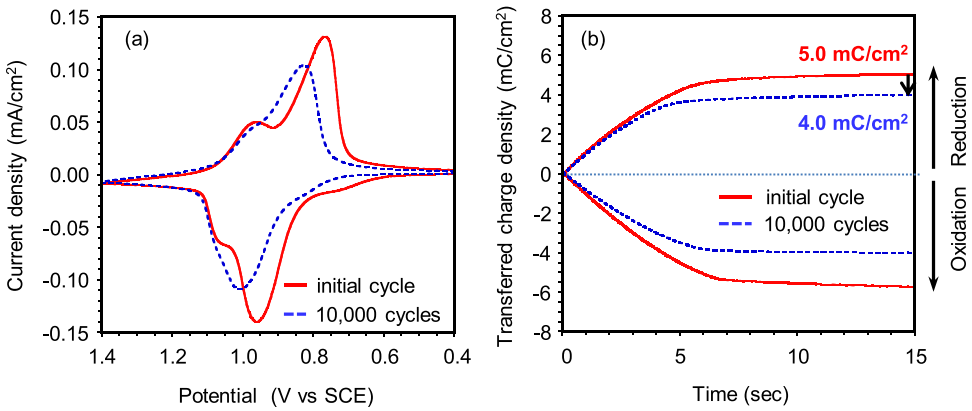

FIG. 4. Cycle stability of the ZnPBA-NP with 20,000 g ($d_{avg} = 58.8$ nm): (a) cyclic voltammograms for initial and 10 000th cycles and (b) transferred charge density during chronocoulometry for the initial and 10 000th cycles.

regarded as very promising materials for use as counterelectrodes of PB ECDs.

Zn-PBA (zinc hexacyanoferrate) nanoparticles smaller than 100 nm were prepared using ultracentrifuge processing at 9000–20 000 g. The current density and transferred charge density of the Zn-PBA films increased with the decrease of the particle size because of the increased surface area. The largest current density and the maximum transferred charge density of 5.0 mC/cm^2 were obtained for the Zn-PBA film with average particle size of 58.8 nm. The film showed stable cycling up to 10 000 cycles. The Zn-PBA nanoparticle films prepared using ultracentrifuge process are regarded as promising candidates for use as counter-electrode materials of PB ECDs.

[1]J. Borratt and K. Dowd, Des. Manage. Rev. **17**(4), 24 (2006).
[2]S. Hara, H. Tanaka, T. Kawamoto, M. Tokumoto, M. Yamada, A. Gotoh, H. Uchida, M. Kurihara, and M. Sakamoto, Jpn. J. Appl. Phys., Part 2 **46**, L945 (2007).
[3]S. Hara, H. Shiozaki, A. Omura, H. Tanaka, T. Kawamoto, M. Tokumoto, M. Yamada, A. Gotoh, M. Kurihara, and M. Sakamoto, Appl. Phys. Express **1**, 104002 (2008).
[4]L. Su, H. Wang, and Z. Lu, Mater. Chem. Phys. **56**, 266 (1998).
[5]T.-H. Kuo, C.-Y. Hsu, K.-M. Lee, and K.-C. Ho, Sol. Energy Mater. Sol. Cells **93**, 1755 (2009).
[6]K.-C. Chen, C.-Y. Hsu, C.-W. Hu, and K.-C. Ho, Sol. Energy Mater. Sol. Cells **95**, 2238 (2011).
[7]J.-H. Kang, S.-M. Paek, S.-J. Hwang, and J.-H. Choy, Electrochem. Commun. **10**, 1785 (2008).
[8]S. A. Agnihotry, P. Singh, A. G. Joshi, D. P. Singh, K. N. Sood, and S. M. Shivaprasad, Electrochim. Acta **51**, 4291 (2006).
[9]S. Pahal, M. Deepa, S. Bhandari, K. N. Sood, and A. K. Srivastava, Sol. Energy Mater. Sol. Cells **94**, 1064 (2010).
[10]M. Ishizaki, A. Gotoh, M. Abe, M. Sakamoto, H. Tanaka, T. Kawamoto, and M. Kurihara, Chem. Lett. **39**, 762 (2010).
[11]S.-F. Hong and L.-C. Chen, Electrochim. Acta **53**, 5306 (2008).
[12]M. Ishizaki, K. Kanaizuka, M. Abe, Y. Hoshi, M. Sakamoto, T. Kawamoto, H. Tanaka, and M. Kurihara, Green Chem. **14**, 1537 (2012).
[13]S.-F. Hong and L.-C. Chen, Electrochim. Acta **55**, 3966 (2010).
[14]S.-F. Hong and L.-C. Chen, Sol. Energy Mater. Sol. Cells **104**, 64 (2012).
[15]A. Gotoh, H. Uchida, M. Ishizaki, T. Satoh, S. Kaga, S. Okamoto, M. Ohta, M. Sakamoto, T. Kawamoto, H. Tanaka, M. Tokumoto, S. Hara, H. Shiozaki, M. Yamada, M. Miyake, and M. Kurihara, Nanotechnology **18**, 345609 (2007).
[16]D. M. Delongchamp and P. T. Hammond, Adv. Funct. Mater. **14**, 224 (2004).
[17]H. Shiozaki, T. Kawamoto, H. Tanaka, S. Hara, M. Tokumoto, A. Gotoh, T. Satoh, M. Ishizaki, M. Kurihara, and M. Sakamoto, Jpn. J. Appl. Phys., Part 1 **47**, 1242 (2008).
[18]A. Eftekhari, J. Electroanal. Chem. **537**, 59 (2002).